

Off equilibrium dynamics in 2d-XY system

Stéphane Abriet and Dragi Karevski

Laboratoire de Physique des Matériaux, UMR CNRS No. 7556, Université Henri Poincaré (Nancy 1), B.P. 239, F-54506 Vandœuvre lès Nancy cedex, France

September 15, 2003

Abstract. We study the non-equilibrium time evolution of the classical XY spin model in two dimensions. The two-time autocorrelation and linear response functions are considered for systems initially prepared in a high temperature state and in a completely ordered state. After a quench into the critical phase, we determine, via Monte Carlo simulations, the time-evolution of these quantities and extract the temperature dependence of the slope of the parametric plot susceptibility/correlation in the asymptotic regime. This slope is usually identified with the infinite fluctuation-dissipation ratio which measures the violation to the equilibrium fluctuation-dissipation theorem. However, a direct measure of this ratio leads to a vanishing value.

PACS. 75.40.Gb Dynamic properties
05.70.Ln Non-equilibrium and irreversible thermodynamics

1 Introduction

Non-equilibrium properties of classical spin systems have received a lot of interest these last years, especially in the context of aging[1,2] and from the point of view of fluctuation-dissipation theorem (FDT) and its extensions.[3] The main feature of non-equilibrium dynamics is the breakdown of time-translation invariance, which is a characteristic that has been used recently, together with space-symmetries in order to build a space-time conformal like theory for some scale invariant systems.[4] This theory has given some predictions that have been already tested on some systems, like the Ising with Glauber dynamics or spherical model.[5] A system relaxing towards its equilibrium state shows, in the aging regime, a dependence in the two-time functions on both the observation time t and the so called waiting time $t_w < t$. In this context, an extension of the fluctuation-dissipation theorem (FDT) was proposed.[6] At equilibrium, the FDT relates the correlation function to its conjugate linear response function via

$$R(t - t_w) = \beta \frac{\partial}{\partial t_w} C(t - t_w), \quad (1)$$

where the time enters only through the difference $t - t_w$. Out of equilibrium, the generalisation takes the form

$$R(t, t_w) = X(t, t_w) \beta \frac{\partial}{\partial t_w} C(t, t_w), \quad (2)$$

defining the factor $X(t, t_w)$, the so called fluctuation-dissipation ratio which measures the violation of the FDT.

It measures the ratio between the actual response and the expected response if the FDT was valid. Recently, a lot of interest was put in the asymptotic value of the FDT ratio, defined by

$$X_\infty = \lim_{t_w \rightarrow \infty} \lim_{t \rightarrow \infty} X(t, t_w). \quad (3)$$

In particular, Godrèche and Luck[7] proposed that this quantity should be universal for a critical quench. Evidences to support this universality were obtained on exactly solvable spin systems quenched from infinite temperature, numerically on 2d and 3d Ising model with Glauber dynamics[8] and also checked from field-theoretic two-loop expansion of the $O(n)$ model[9] and the 2d voter model.[10] This universality was tested recently for a wide class of initial states in 1d Glauber Ising model.[11]

However, going on more complex systems the linear response function itself is not accessible by numerical, nor experimental analyses and one is forced to look on integrated response functions, that is measuring susceptibilities:

$$\chi(t, t_w) = \int_{t_w}^t dt' R(t, t'), \quad (4)$$

where the perturbation field is applied between time t_w and t , that is a zero-field-cooled (ZFC) scenario. To extract information from the susceptibility on the FDT ratio, one usually plots the susceptibility versus the correlation function and defines from the asymptotic slope of the curve, a number

$$X_\infty^\chi = - \lim_{C \rightarrow 0} \frac{d\chi}{dC} \quad (5)$$

which is often identified with the FDT ratio X_∞ . The idea behind that is coming from the analyses of infinite-range glassy systems[12] where asymptotically, the fluctuation-dissipation ratio depends on time only through the correlation function. One has for those systems

$$X(t, t_w) = X(C(t, t_w)). \quad (6)$$

In this context, the limiting ratio X_∞ was interpreted as a temperature ratio between the actual inverse temperature β and an effective inverse temperature seen by the system:[14] $\beta_{eff} = \beta X$. From the dependence (6), one obtains for the susceptibility the expression

$$\chi(t, t_w) = \beta \int_{C(t, t_w)}^1 dC' X(C'). \quad (7)$$

This last equation strictly holds if the violation ratio is a function of $C(t, t_w)$ only and in this case, one can identify X_∞ with X_∞^χ . It is in particular the case at equilibrium since $X = 1$ is a pure constant and it gives $\chi = \beta(1 - C)$.

In a recent work, [15] an exact expression was derived for Glauber-like dynamics which enables to calculate directly the linear response function to an infinitesimal field. The advantage of this approach is obvious since it gives direct access to the linear response, non-linear effects are avoided, and not only to the susceptibility as in the ZFC scenario.

In this context, we have performed a Monte Carlo study of the nonequilibrium evolution of the two-dimensional classical XY system. We have studied the evolution of the system after a quench from infinite temperature toward the low temperature critical phase, up to the Kosterlitz-Thouless point. We have also considered the relaxation from a completely ordered initial state. For that purpose, we have calculated two-point correlation functions, susceptibilities and response functions. From these data, we have checked the violation of the FDT and compared our numerics with theoretical predictions (spin wave approximation) and previous numerical works when available. The paper is organised as follows: in the next section, we present the dynamics of the model and its solution for two-time quantities in the spin wave approximation. The following section deals with the numerical analyses for the ordered initial state. We turn then to the infinite temperature initial condition. We summarise and discuss our results in the last section.

2 Two-dimensional dynamical XY model

The two-dimensional ferromagnetic XY model is defined via the Hamiltonian

$$H = - \sum_{\langle ij \rangle} S_i \cdot S_j \quad (8)$$

where the sum is over nearest neighbour pairs ij on a square lattice and where the classical spin variables S_i are two-dimensional vector fields of unit length. Introducing

angular variables, one can rewrite the original Hamiltonian in the form

$$H = - \sum_{\langle ij \rangle} \cos(\theta_i - \theta_j). \quad (9)$$

The equilibrium properties of this model are well-known since the pioneering work of Berezinskii,[16] Kosterlitz and Thouless and others.[17] At a temperature T_{KT} , the system undergoes a continuous topological transition due to the pairing of vortex and anti-vortex excitations. Below the transition temperature, the system is characterised by a line of critical points reflecting a quasi-long range ordered phase with algebraic correlation functions. The spin-spin correlation critical exponent η is continuously varying with the temperature field. Although for the spin-spin η exponent spin-wave approximation gives an accurate analytic prediction at low temperature,[16] only numerical estimates are known for the full temperature regime.[18]

The dynamics of the model was studied extensively in the context of coarsening.[19] The two-time spin-spin autocorrelation function and the associated linear response function have been studied only recently in ref.[20]. In the spin-wave approximation, valid at low temperature ($T \ll T_{KT} \simeq 0.89$), the nonconserved dynamics of the angular variable is given by the Langevin equation[19]

$$\frac{\partial}{\partial t} \theta(x, t) = - \frac{\delta F(\theta)}{\delta \theta} + \zeta(x, t) \quad (10)$$

where $\zeta(x, t)$ is a Gaussian thermal noise with variance $\langle \zeta(x, t) \zeta(x', t') \rangle = 2T\delta(x - x')\delta(t - t')$ and the free energy functional is given by[19]

$$F(\theta) = \frac{\rho(T)}{2} \int d^2x [\nabla \theta]^2 \quad (11)$$

where $\rho(T)$ is the spin-wave stiffness, related to the $\eta(T)$ exponent by the relation $2\pi\rho(T) = T/\eta(T)$.

Taking as initial condition a completely ordered state $\theta(x, 0) = \theta_0$, using the previously defined spin-wave functional, it is possible to obtain analytical expressions for the two-time autocorrelation and response functions. These reads, at enough long times, for the autocorrelation function $C(t, t_w) = V^{-1} \int d^2x \langle \cos[\theta(x, t) - \theta(x, t_w)] \rangle$:[20]

$$C(t, t_w) = \frac{1}{(t - t_w)^{\eta(T)/2}} \left(\frac{(1 + \lambda)^2}{4\lambda} \right)^{\eta(T)/4}, \quad (12)$$

where t_w is the waiting time, t is the total time and $\lambda = t/t_w$ is the scaling ratio. This behaviour can be explained in the following way. At short time difference $t - t_w \ll t_w$, the fluctuations of small wavelength ($\ll \xi(t_w)$) have equilibrated and we are in a quasi-equilibrium regime with a correlation function decaying as $C(t, t_w) \sim (t - t_w)^{-\eta(T)/z}$ where the dynamical exponent $z = 2$ for the 2d XY model. At longer times, when the scaling function significantly differs from 1, the aging process takes place giving rise to a full two-time dependence, that is a breakdown of time-translation invariance. The conjugate response function,

defined by $R(t, t_w) = V^{-1} \int d^2x \frac{\delta \langle S(x, t) \rangle}{\delta h(x, t_w)} \Big|_{h=0}$ is

$$R(t, t_w) = \frac{2\eta(T)}{T} \frac{C(t, t_w)}{t - t_w}, \quad (13)$$

with $C(t, t_w)$ given in equation (12). It is amazing to notice at this point that the last equation has exactly the form obtained from the Fluctuation-Dissipation theorem with a power law equilibrium correlation function $C(t, t_w) \simeq A(t - t_w)^{-\eta/z}$, where z is the dynamical exponent. The difference from the equilibrium situation lies in the fact that the nonequilibrium amplitude A is actually depending on time too. So, by differentiation, one has also a term arising from the derivative of the amplitude $A(t_w)$, leading to a deviation from the FDT. From equations (12) and (13), it is easy together with the definition of the fluctuation-dissipation ratio given previously to obtain

$$X(t, t_w) = \left(1 - \frac{(\lambda - 1)^2}{2(1 + \lambda)}\right)^{-1}. \quad (14)$$

For a quench from an infinite temperature state to a temperature $T < T_{KT}$, no such analytical expressions are available. However, on the basis of scaling arguments,[19] one can postulate the general expressions

$$C(t, t_w) = \frac{1}{(t - t_w)^{\eta(T)/2}} f_C \left(\frac{\xi(t)}{\xi(t_w)} \right) \quad (15)$$

and

$$R(t, t_w) = \frac{1}{(t - t_w)^{1+\eta(T)/2}} f_R \left(\frac{\xi(t)}{\xi(t_w)} \right) \quad (16)$$

where f_C and f_R are the scaling function and where the correlation length ξ has a different behaviour if the quench is done from infinite temperature or from a completely ordered initial state, namely one has:[21]

$$\xi(t) \sim \begin{cases} t^{1/2} & T_i < T_{KT} \\ (t/\ln t)^{1/2} & T_i > T_{KT} \end{cases} \quad (17)$$

The logarithmic correction in the disordered initial state case is due to the slowing down of the coarsening caused by the presence of free vortices,[21] since the approach toward equilibrium proceeds through the annihilation of vortex-antivortex pairs, a process which is slower than the equilibration of spin waves.

We shall concentrate first on checking numerically these analytical predictions, testing at the same time the validity of our numerics, and then turn to the numerical study of the infinite-temperature initial condition.

3 Numerics

3.1 Numerical approach

During the simulations, the system is initially prepared in two different ways: spin angles θ_i chosen at random in the

interval $[0, 2\pi]$ corresponding to the infinite temperature initial state and constant initial angles, $\theta_i = cst$. $\forall i$, corresponding to the zero temperature initial state. For the numerical analysis, we use a standard metropolis dynamics where a spin chosen at random is turned at random with an acceptance probability given by $\min[1, \exp(-\Delta E/T)]$ where ΔE is the difference energy between the actual configuration and the former one. As stated before, in order to go beyond the susceptibility and to access directly the response itself, we use a different dynamics, Glauber-like, where the transition probabilities of a configuration with a spin S_i to a new value S'_i is given by

$$p(S_i \rightarrow S'_i) = \frac{W(S'_i)}{W(S'_i) + W(S_i)} \quad (18)$$

with

$$W(S_i) = \exp \left(-\frac{1}{T} S_i \sum_j S_j \right). \quad (19)$$

Both dynamics have the same dynamical exponents and one expect no significant changes for thermodynamical quantities.

The two-times autocorrelation function is defined by

$$C(t, t_w) = \frac{1}{L^2} \sum_i \langle \cos[\theta_i(t) - \theta_i(t_w)] \rangle \quad (20)$$

where $\langle \cdot \rangle$ is the average over the thermal histories. In the metropolis simulation, we calculate the ZFC susceptibility via[22]

$$\chi(t, t_w) = \frac{1}{L^2 h^2} \sum_i \overline{\langle h_i \cdot S_i(t) \rangle} \quad (21)$$

where h is a small bimodal random magnetic field applied from t_w . The overline means an average over the field realizations. Practically in our simulations we use the value $h = 0.04$.[23]

The response function itself is obtained numerically with the help of the Glauber-like dynamics.[15] By definition, the autoresponse to an infinitesimal magnetic field applied at t_w is given by

$$R(t, t_w) = \frac{\delta S_i(t)}{\delta h_i(t_w)}. \quad (22)$$

With the help of the master equation

$$P(\{\theta'\}, t + 1) = \sum_{\{\theta\}} p(\{\theta\} \rightarrow \{\theta'\}) P(\{\theta\}, t) \quad (23)$$

and following the lines of ref.[15], it is easy to arrive at

$$R(t, t_w) = \beta \langle \cos \theta_i(t) [\cos \theta_i(t_w + 1) - \cos \theta_i^w(t_w + 1)] \rangle + \beta \langle \sin \theta_i(t) [\sin \theta_i(t_w + 1) - \sin \theta_i^w(t_w + 1)] \rangle \quad (24)$$

where $\cos \theta_i^w(t)$ and $\sin \theta_i^w(t)$ are the components of the Weiss magnetisation given by

$$S_i^{x,y} = \frac{1}{\beta} \frac{\partial}{\partial h_{x,y}} \ln Z_i \Big|_{h=0}. \quad (25)$$

$Z_i = \exp(-\beta H(\theta_i, h)) + \exp(-\beta H(\theta'_i, h))$ is the local partition function in the field.

The thermodynamical quantities are calculated on square samples with periodic boundary conditions of linear size up to $L = 512$ and averaged typically over 1000 thermal histories.

3.2 Ordered initial state

We start with a completely ordered state and set the temperature $T < T_{KT}$, in order first to check the compatibility of our numerics with the analytical predictions in the spin-wave approximation. In figure 1, we present the results obtained for the autocorrelation function in the asymptotic regime $t - t_w \gg t_w \gg 1$ for a temperature of $T = 0.3$ where the expression (12) is expected to hold. For different waiting times, the collapse of the data is fairly good and the power-law behaviour in terms of the variable $(1 + \lambda)^2/(4\lambda)$ gives a very good agreement with the XY $\eta(T)$ exponent, as it can be seen on figure 2.

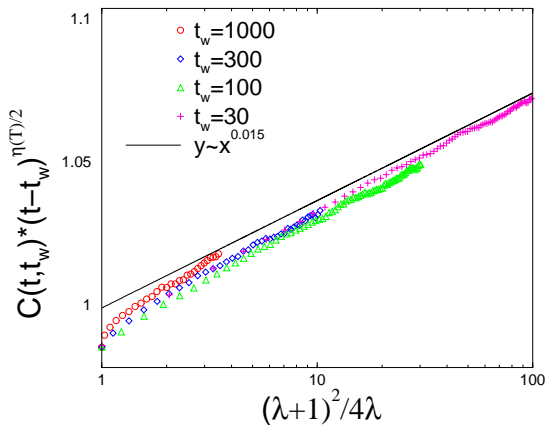


Fig. 1. Rescaled autocorrelation function at $T = 0.3$ for a system of linear size $L = 512$ and for different waiting times. The solid line is guide for the eyes corresponding to the value $\eta(0.3) \simeq 0.015$.

In the asymptotic regime, the two-times response function is expected to be given, at least at low temperature by the spin-wave approximation formula (13). In figure 3, we give the numerical results obtained for a final temperature of $T = 0.3$ for different waiting times. The aging part of the response is very small in the accessible regime and the deviation from a time-invariant process is very difficult to be seen as the collapse of the data for different waiting times in figure 3 attests. Nevertheless, we have plotted in figure 4 directly the numerical response function together with the analytical prediction. The superposition of both curves seems to validate the expected law. Although, in ref.[20] this case was considered quite extensively, it was done only for one temperature. Here we have extended the results to the whole low temperature regime.

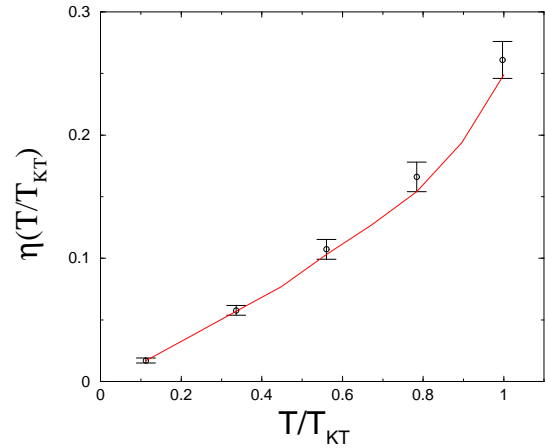


Fig. 2. Dependence of the η exponent on temperature extracted from the two-time autocorrelation function (symbols). The solid line corresponds to numerical values given in ref.[18].

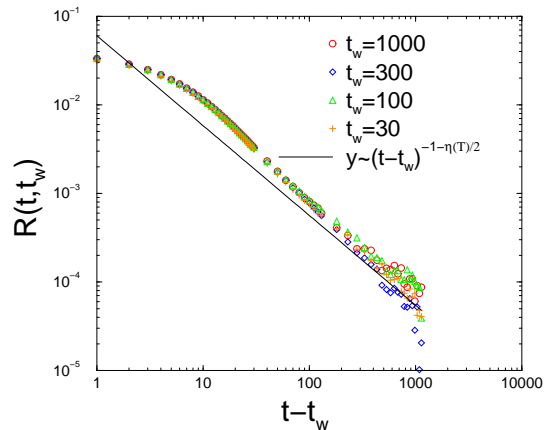


Fig. 3. Response function at $T = 0.3$ for different waiting times.

3.3 Infinite temperature initial state

The infinite-temperature initial state is more canonical in the study of coarsening and aging effects. After the quench in the critical phase, the correlation length will grow in time with a logarithmic correction due to the interaction of walls with free vortices as mentioned in ref.[21]. That is, $\xi(t) \sim (t / \ln t)^{1/2}$ and leading to the conjectures (15,16) for the correlation and response functions. Berthier *et al* have checked this conjecture for the correlation length only for one final temperature, namely $T = 0.3$. In figure 5 we show the results obtained for several quench temperatures, ranging from $T = 0.1$ up to $T = 0.7$. The collapse of the rescaled correlation functions $(t - t_w)^{\eta/2} C(t, t_w)$ as function of the variable $\xi(t)/\xi(t_w)$ is very satisfactory. From these curves, we can extract the scaling function f_C , see equation (15), and find the power law behaviour $f_C(x) \sim x^{-\kappa}$ with a temperature independent exponent $\kappa = 1.05(10)$. In ref.[20] the value $\kappa = 1.08$ was given

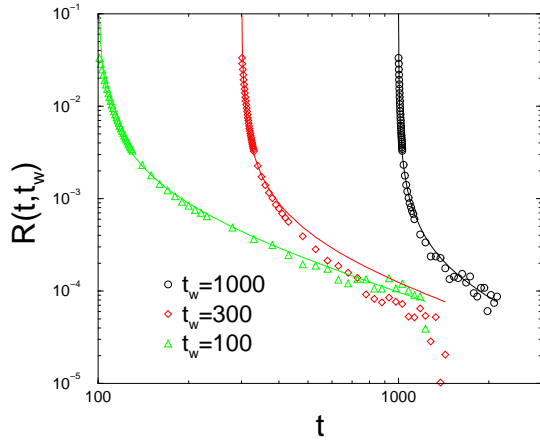


Fig. 4. Response function for different waiting times for a system of linear size $L = 512$. The quench temperature is $T = 0.3$. The different waiting time curves are collapsing and lead to the equilibrium value $R(t, t_w) = 1$, they have a constant slope, R_∞^X , independent of t_w . This number R_∞^X corresponds, when $R(t, t_w) = R(C(t, t_w))$ only, to the asymptotic limit $R_\infty = \lim_{t_w \rightarrow \infty} \lim_{t \rightarrow \infty} R(t, t_w)$. In figure 6, where we have represented R_∞^X versus the reduced temperature T/T_{KT} , we clearly see a linear behaviour, starting at $R_\infty^X = 0$ for $T = 0$ and finishing at the value $R_\infty^X = 1/2$ at the Kosterlitz-Thouless point. It can be noticed that this continuous dependence of the FDT ratio on a model parameter was also observed in the spherical model.[24]

which is of course compatible with our data. However,

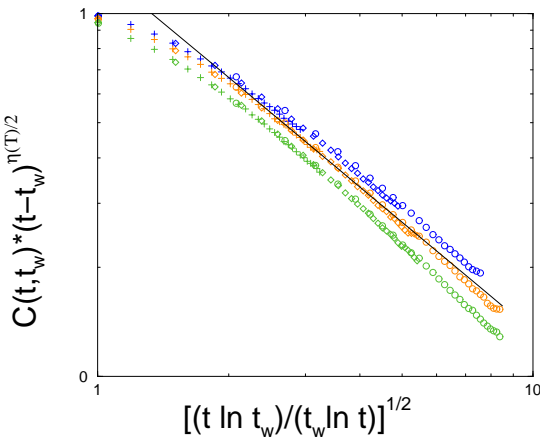


Fig. 5. Scaling plot of the two-times autocorrelation function for a quench from infinite temperature towards $T < T_{KT}$. The three different collapsed curves are obtained for $T = 0.3$, $T = 0.5$ and $T = 0.7$ from top to bottom. The different waiting times for each temperature are $t_w = 100$ circles, $t_w = 300$ diamonds and $t_w = 1000$ crosses. The solid line corresponds to $1/x$.

one has to be careful in this statement since the exponent is very close to 1. For example, if one takes as the scaling variable $x^{-1} = \xi(t_w)/\xi(t)$ instead of $x = \xi(t)/\xi(t_w)$, then the scaling limit we are interested in is $x^{-1} \ll 1$ and what is seen could be very possibly the leading expansion terms of an analytical scaling function, that is $g(x^{-1}) \simeq g(0) + \alpha x^{-1}$. Moreover, numerically the extrapolated value $g(0)$ seems to be very close to zero (less than 0.01) and it is impossible to test this value in the time range explored in this work. The same is true for the reference [20]. So if $g(0)$ is not vanishing, finally at long enough

times, the decay of the autocorrelation function has the same power law dependence as in the equilibrium situation. Otherwise, the decay is faster with a power law $t^{-\eta/2-1/2}$ up to logarithmic corrections.

The parametric plot of the susceptibility times the temperature versus the correlation function does not collapse for different waiting times, showing that the fluctuation-dissipation ratio is not a function of C only but rather has a dependence on both t and t_w . However, after an initial quasi-equilibrium regime, where the different waiting time curves are collapsing and lead to the equilibrium value $X(t, t_w) = 1$, they have a constant slope, X_∞^X , independent of t_w . This number X_∞^X corresponds, when $X(t, t_w) = X(C(t, t_w))$ only, to the asymptotic limit $X_\infty^X = \lim_{t_w \rightarrow \infty} \lim_{t \rightarrow \infty} X(t, t_w)$. In figure 6, where we have represented X_∞^X versus the reduced temperature T/T_{KT} , we clearly see a linear behaviour, starting at $X_\infty^X = 0$ for $T = 0$ and finishing at the value $X_\infty^X = 1/2$ at the Kosterlitz-Thouless point. It can be noticed that this continuous dependence of the FDT ratio on a model parameter was also observed in the spherical model.[24]

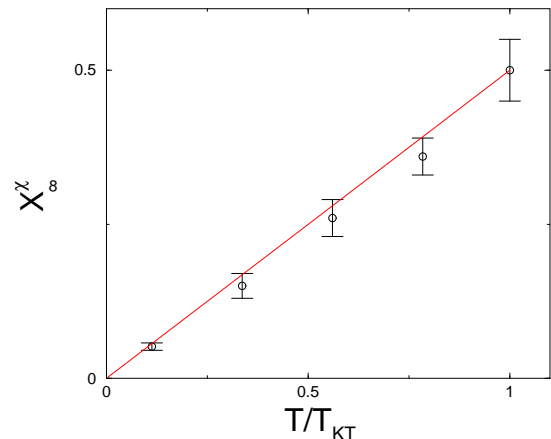


Fig. 6. Fluctuation-dissipation ratio versus reduced temperature T/T_{KT} . The line is the conjectured function.

Finally, we present the data obtained for the linear response function and the fluctuation-dissipation ratio $X(t, t_w)$. The simulations are done on lattices of linear size up to $L = 100$ averaged over 11000 realizations in order to have a good enough statistics for X . In figure 7, we show the result obtained for a final temperature $T = 0.1$. Very similar curves are obtained for other temperatures. The collapse of the data for different waiting times is very good, which confirms the scaling conjecture (16). Although the number of different histories we have realized is quite huge, the noise on the points is still important. The range of time used is from $t = 100$ up to $t = 2500$, which explains the very short window of the x-axis in figure 7. Nevertheless, what is seen after an initial short time regime is a linear behaviour in terms of the scaling variable $\xi(t)/\xi(t_w)$, that

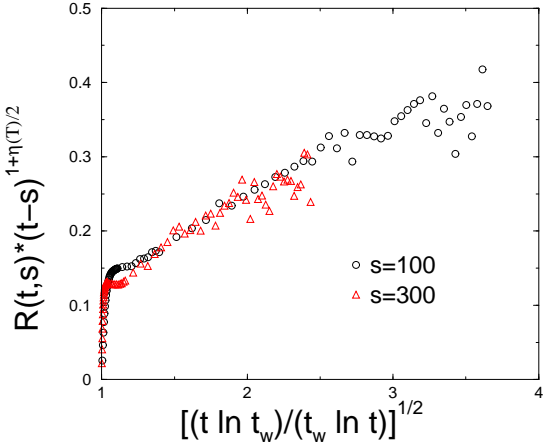


Fig. 7. Rescaled response function at $T = 0.1$ for a linear system size $L = 100$ averaged over 11000 realizations.

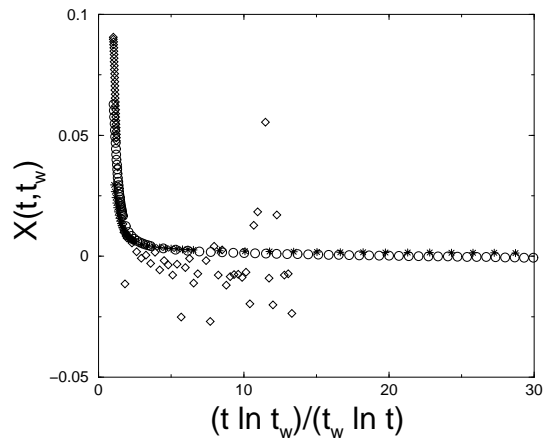


Fig. 8. Fluctuation-dissipation ratio at $T = 0.1$ as a function of the scaling variable $t \ln t_w / t_w \ln t$ for $t_w = 10$ (stars), $t_w = 30$ (circles) and $t_w = 100$ (diamonds).

is asymptotically

$$(t - t_w)^{1+\eta/2} R(t, t_w) \simeq A_R \left(\frac{t \ln t_w}{t_w \ln t} \right)^{1/2}, \quad (26)$$

with an amplitude A_R slowly varying with the temperature. In figure 8, we present the fluctuation-dissipation ratio $X(t, t_w)$ as a function of $t \ln t_w / t_w \ln t$ obtained numerically at the same temperature, $T = 0.1$, for waiting times $t = 10, 30, 100$. Since in the calculation of X , we have to do a derivative, the results obtained are much more noisy and it is difficult to go on very long waiting times. Nevertheless, we clearly see a good collapse on a master curve, leading to a vanishing fluctuation-dissipation ratio in the asymptotic limit. The same is obtained for other temperatures.

4 Summary and outlook

We have studied numerically the non-equilibrium relaxation properties of the two-dimensional XY model initially prepared on two distinct ways: completely ordered and fully disordered state. In both cases, the two-time spin autocorrelation function and the associated linear response function were determined.

In the initial ordered case, we have fully confirmed the analytical predictions obtained in the spin wave approximation, strictly valid at very low temperature. Nevertheless, the scaling form given in equation (12) seems to be valid in a wide range of temperature below the Kosterlitz-Thouless transition. From it, we have extracted the equilibrium exponent $\eta(T)$ with a quite good accuracy as seen in figure 2. Using the Glauber-like dynamics defined previously, we have obtained directly the linear response function itself. This permits a direct comparison of our data with the analytical expression (13). With this approach, we avoided difficulties inherent in the use of susceptibilities, which can be affected by short-time contributions. Although the aging part of the response seems to be very small, as attested in figure 3, the plot in figure 4 shows a very good agreement between the numerical data and the analytical prediction.

Starting with a fully disordered state, we have extended the conjecture checked in ref.[20] for one particular temperature to the whole low temperature regime. For temperature ranging from $T = 0.1$ up to $T = 0.9$, we have numerically confirmed the forms (15) and (16) of the correlation and response functions with a scaling variable given in (17). As discussed previously, we found numerically for the asymptotic behaviour of the autocorrelation scaling function f_C , defined in (16), a behaviour which is compatible with a purely algebraic decay with a temperature independent exponent very close to one. The linear response scaling function, in the time-range studied here, has a linear behaviour in the scaling variable $\xi(t)/\xi(t_w)$. Those asymptotic behaviours of the correlation and response scaling functions are supporting, up to logarithmic factors, the forms given by local scale-invariance theory.[4] Utilising the notations of [8], one has

$$C(t, t_w) \simeq t_w^{-a} F_C(t/t_w) \quad (27)$$

$$R(t, t_w) \simeq t_w^{-a-1} F_R(t/t_w), \quad (28)$$

where the scaling functions F_C and F_R have the asymptotic forms

$$F_{C,R}(u) \simeq A_{C,R} u^{-\lambda_{C,R}/z} \quad u \gg 1. \quad (29)$$

From our data, we obtain $a = \eta(T)/2$ and $\lambda_C = \lambda_R = \eta(T) + 1$ confirming the general scenario depicted in ref.[4, 8, 25]. Finally, we extracted X_∞^X , from the parametric susceptibility/correlation plot in the long-time limit. The result we obtained is well fitted by the linear behaviour $X_\infty^X = (1/2)T/T_{KT}$. The direct use of the response function gave a different answer, as seen in figure 8. Although the fluctuation-dissipation ratio $X(t, t_w)$ is a function of both t and t_w , this dependence seems to enter only

through the scaling ratio $t \ln t_w / t_w \ln t$. From the numerical results we obtained on the correlation and response functions, it is clear that in the asymptotic regime the fluctuation dissipation ratio $X_\infty = \lim_{t_w \rightarrow \infty} \lim_{t \rightarrow \infty} X(t, t_w)$ is vanishing. A result which is different from what is obtained from the parametric susceptibility/correlation plot. This vanishing is due to the breakdown of scaling induced by the presence of the logarithmic factors in the scaling functions. In practice, one has to take care when discussing those plots, especially when no master curve is ever reached for different waiting times.

Acknowledgments

Thanks to C. Chatelain and M. Henkel for the support they offered to us. The other members of the Groupe de Physique Statistique are greatfully acknowledged too.

References

1. J.-P. Bouchaud, L. F. Cugliandolo, J. Kurchan and M. Mézard, in *Spin Glasses and Random Fields*, Ed. A. P. Young (World Scientific, Singapore, 1998)
2. A. Crisanti and F. Ritort, *J. Phys. A* **36**, R181 (2003)
3. L. F. Cugliandolo and J. Kurchan, *Phys. Rev. Lett.* **71**, 173 (1993); *J. Phys. A* **27**, 5749 (1994)
4. M. Henkel, *Nucl. Phys.* **B641**, 405-486 (2002)
5. M. Henkel, M. Pleimling, C. Godreche and J.-M. Luck, *Phys. Rev. Lett.* **87**, 265701 (2001); for a recent review see M. Henkel, A. Picone, M. Pleimling and J. Unterberger, [cond-mat/0307649](https://arxiv.org/abs/cond-mat/0307649)
6. L. F. Cugliandolo, J. Kurchan and G. Parisi, *J. Physique I* **14**, 1641 (1994)
7. C. Godrèche and J.-M. Luck, *J. Phys. A* **33**, 1151 (2000); *J. Phys. A* **33**, 9141 (2000)
8. For a recent review see C. Godrèche and J.-M. Luck, *J. Phys. Cond. Matt.* **14**, 1589 (2002)
9. P. Calabrese and A. Gambassi, *Phys. Rev. E* **65**, 066120 (2002); *Phys. Rev. E* **66**, 212407 (2002)
10. F. Sastre, I. Dornic and H. Chaté, [cond-mat/0308178](https://arxiv.org/abs/cond-mat/0308178)
11. M. Henkel and G. M. Schütz, [cond-mat/0308466](https://arxiv.org/abs/cond-mat/0308466)
12. L. F. Cugliandolo, [cond-mat/0210312](https://arxiv.org/abs/cond-mat/0210312)
13. E. Lippiello and M. Zannetti, *Phys. Rev. E* **61**, 3369 (2000)
14. L. F. Cugliandolo, J. Kurchan and L. Peliti, *Phys. Rev. E* **55**, 3898 (1997)
15. C. Chatelain, [cond-mat/0303545](https://arxiv.org/abs/cond-mat/0303545); F. Ricci-Tersenghi, [cond-mat/0307565](https://arxiv.org/abs/cond-mat/0307565)
16. V. L. Berezinskii, *Sov. Phys. JETP* **32**, 493 (1971)
17. J. M. Kosterlitz and D. J. Thouless, *J. Phys. C* **6**1181 (1973); J. M. Kosterlitz, *J. Phys. C* **7**,1046 (1974); J. Villain, *J. Physique* **36**, 581 (1975)
18. B. Berche, *J. Phys. A* **36**, 585 (2003)
19. A. J. Bray, *Adv. Phys.* **43**, 357 (1994)
20. L. Berthier, P. C. W. Holdsworth and M. Sellitto, *J. Phys. A* **34**, 1805 (2001)
21. A. J. Bray, A. J. Briant and D. K. Jervis, *Phys. Rev. Lett.* **84**, 1503 (2000)
22. A. Barrat, *Phys. Rev. E* **57**, 3629 (1998)
23. We take the same value as in Ref. [20] in order to have a direct comparison of our results with those of Berthier *et al.*
24. A. Picone and M. Henkel, *J. Phys. A* **35**, 5575 (2002)
25. M. Henkel, M. Paessens and M. Pleimling, *Europhys. Lett.* **62**, 664 (2003)